

Figure 1. Temperature-programmed reaction spectra resulting from the adsorption of a saturation dose of furan on partially sulfided Mo(100) ($\theta_S = 0.2$ ML), showing the signals corresponding to $m/e = 2$ (di-hydrogen), 28 (carbon monoxide) and 39 and 69 (furan). Adsorption took place at 273 K, and the heating rate was 10 K/s. The partial pressures were uncorrected for differences in ionization efficiency and transmission in the mass spectrometer.

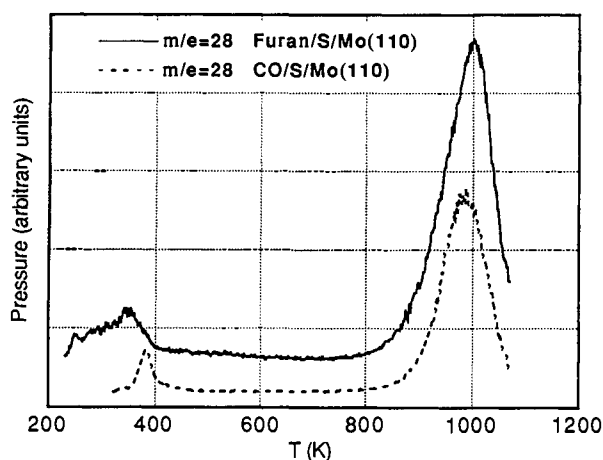
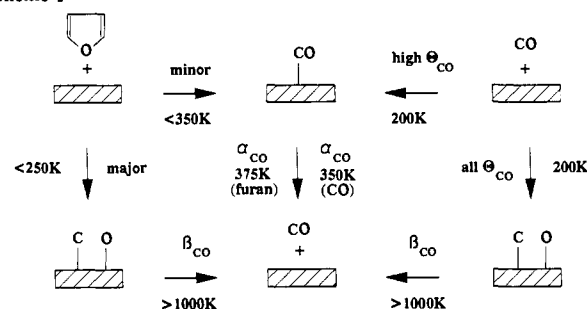


Figure 2. Temperature-programmed reaction spectra for $m/e = 28$ resulting from the adsorption of furan and CO on partially sulfided Mo(100) ($\theta_S = 0.2$ ML) under the same conditions as Figure 1.

perature 28 amu desorption peak commences at a temperature at which all of the molecularly adsorbed furan has already desorbed. Hence this 28 amu signal most probably arises from the production of carbon monoxide or ethylene on the surface. A careful examination of masses corresponding to all of the possible cracking products from these materials showed that this entire spectrum is in fact attributable to CO desorption from adsorbed furan.

The 28 amu TPRS data for the CO/Mo(110) spectrum shown in Figure 2 contains two peaks. The low-temperature peak only appears at high coverages of CO and is attributed to first-order desorption of molecularly bound α -CO. The high-temperature β peak is interpreted as a recombination of C and O atoms from dissociated CO.^{6,7} The 28 amu trace for furan/Mo also exhibits these two features at desorption temperatures very similar to those observed for adsorbed CO. The similarity of the major 28 amu peaks from furan adsorption to those seen from CO adsorption leads us to the conclusion that, while a substantial amount of furan does indeed decompose to give atomic carbon and oxygen on the surface, which later desorbs as β -CO, a direct CO abstraction route also occurs at low temperatures close to 350 K. The CO released from the furan molecule during this process is then immediately

Scheme I



desorbed, as it is above the normal α -CO desorption temperature (Scheme I).

We find support for this type of reaction chemistry in gas-phase pyrolysis experiments.⁸ Here it is found that ring-opening of furan to form a stabilized biradical that subsequently decomposes into propyne and CO is a favored low-energy reaction pathway. Such a mechanism may apply here to furan that has become bonded to the surface through loss of an α -H. There are also parallels with the complex reported by Vollhardt⁹ in which a THF-like species is α -C bonded to Mo as a Fischer carbene, which decomposes to propene and a CO ligand bonded to the Mo.

This low-temperature direct abstraction of CO from furan, though a minority reaction on these surfaces, stands in contrast to the complete retention of sulfur from thiophene on the same surface. Though a surprising reaction at first sight, in hindsight the possibility of forming a stable gas-phase product in the case of furan, but not in the case of thiophene, provides an obvious driving force for this differing behavior.

Acknowledgment. This work was supported by the U.S. Department of Energy, Office of Fossil Energy, Grant DE-FG22-89PC89783. We thank a reviewer for pointing out ref 9.

(8) Grela, M. A.; Amorebieta, V. T.; Colussi, A. J. *J. Phys. Chem.* **1985**, *89*, 38-41.

(9) Drage, J. S.; Vollhardt, K. P. *Organometallics* **1985**, *4*, 191-192.

Real-Time Analysis of Chemical Reactions Occurring at a Surface-Confined Organic Monolayer

Li Sun, Ross C. Thomas, and Richard M. Crooks*

Department of Chemistry and the
Center for High Technology Materials
University of New Mexico
Albuquerque, New Mexico 87131

Antonio J. Ricco*

Microsensor Division 1163, Sandia National Laboratories
Albuquerque, New Mexico 87185

Received June 20, 1991

Revised Manuscript Received August 29, 1991

We report the first real-time measurements of a chemical reaction between a surface-confined organic monolayer and a vapor-phase reactant.¹ To demonstrate monolayer reaction

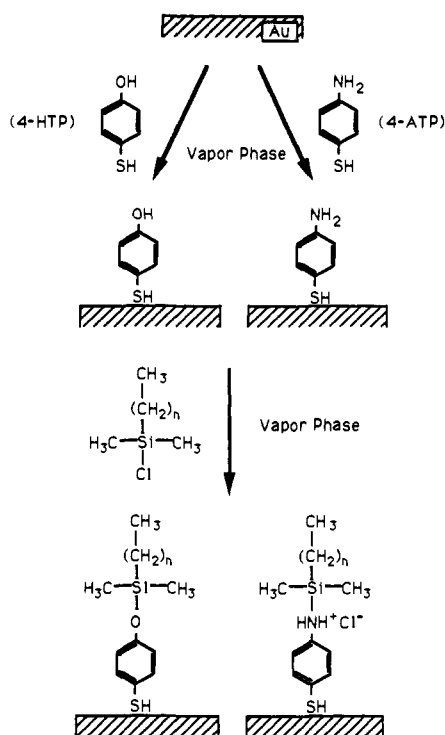
* Authors to whom correspondence should be addressed.

(1) Surface reactions similar to those reported here have been previously carried out in solution by, first, Sagiv and, in elegant recent examples, Mallouk, Ulman, Whitesides, and Marks and Ratner. See: (a) Pomerantz, M.; Segmuller, A.; Netzer, L.; Sagiv, J. *Thin Solid Films* **1985**, *132*, 153. (b) Gun, J.; Iscovici, R.; Sagiv, J. *J. Colloid Interface Sci.* **1984**, *101*, 201. (c) Netzer, L.; Iscovici, R.; Sagiv, J. *Thin Solid Films* **1983**, *100*, 67. (d) Netzer, L.; Iscovici, R.; Sagiv, J. *Thin Solid Films* **1983**, *99*, 235. (e) Lee, H.; Kepley, L. J.; Hong, H.-G.; Mallouk, T. E. *J. Am. Chem. Soc.* **1988**, *110*, 618. (f) Ulman, A.; Tillman, N. *Langmuir* **1989**, *5*, 1418. (g) Ulman, A. *J. Mater. Educ.* **1989**, *11*, 205. (h) Tillman, N.; Ulman, A.; Penner, T. L. *Langmuir* **1989**, *5*, 101. (i) Wasserman, S. R.; Whitesides, G. M.; Tidswell, I. M.; Ocko, B. M.; Pershan, P. S.; Axe, J. D. *J. Am. Chem. Soc.* **1989**, *111*, 5852. (j) Li, D.; Ratner, M. A.; Marks, T. J. *J. Am. Chem. Soc.* **1990**, *112*, 7389.

(6) Zaera, F.; Kollin, E. B.; Gland, J. L. *Chem. Phys. Lett.* **1985**, *121*, 464-468.

(7) Felter, T. E.; Estrup, P. J. *Surf. Sci.* **1978**, *67*, 464-482.

Scheme I



chemistry, we rely on the coupling reaction between surface-confined monolayers^{2,3} of 4-hydroxythiophenol, 4-HTP, or 4-aminothiophenol, 4-ATP, adsorbed on a polycrystalline Au substrate and vapor-phase dimethyloctylchlorosilane, $[\text{CH}_3(\text{C}-\text{H}_2)_7](\text{CH}_3)_2\text{SiCl}$, Scheme I. Results obtained from surface acoustic wave (SAW) devices, Fourier transform infrared-external reflectance spectroscopy (FTIR-ERS), and optical ellipsometry confirm for the first time that precisely stoichiometric coupling between the surface-confined adsorbate and the vapor-phase reactant occurs. The results demonstrate the feasibility of changing the chemical properties of surfaces by means of an in situ, vapor-phase chemical reaction. Surface transformations such as those described here have implications for molecular recognition based chemical sensors and technologies that require surface characteristics to be altered on demand.

We have recently reported the results of a real-time gravimetric analysis of the vapor-phase adsorption of several *n*-alkanethiols onto Au-coated SAW devices.⁴ That strategy is extended here to follow the real-time reaction/adsorption behavior of the coupling reaction between surface-confined 4-HTP or 4-ATP⁵ and $[\text{C}-\text{H}_3(\text{CH}_2)_7](\text{CH}_3)_2\text{SiCl}$. Figure 1 shows a plot of frequency shift versus time for a Au-modified SAW device during sequential exposure to flowing N_2 streams containing 4-ATP and $[\text{CH}_3(\text{C}-\text{H}_2)_7](\text{CH}_3)_2\text{SiCl}$.⁴ Between 0 and 85 min, the device is allowed to stabilize in a flowing purge of pure N_2 ; the frequency drift during this period is a measure of device stability. Between 85 and 240 min the N_2 purge is switched to a 4-ATP/ N_2 vapor stream; the magnitude of the frequency change indicates condensation of 4-ATP multilayers on the surface of the device. From 240 to 410 min a pure N_2 purge is again introduced until the frequency stabilizes at -11.4 ppm or about 153 ng/cm^2 ($1.22 \times 10^{-9} \text{ mol/cm}^2$) of adsorbed 4-ATP, approximately one monolayer.⁶

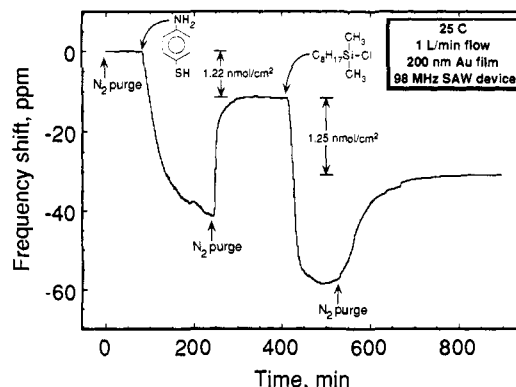


Figure 1. Real-time SAW device response obtained for the adsorption of 4-ATP followed by reaction between surface-confined 4-ATP and $[\text{CH}_3(\text{CH}_2)_7](\text{CH}_3)_2\text{SiCl}$. The final mass change due to 4-ATP adsorption is 153 ng/cm^2 ($1.22 \times 10^{-9} \text{ mol/cm}^2$), and the additional mass change due to $[\text{CH}_3(\text{CH}_2)_7](\text{CH}_3)_2\text{SiCl}$ is 229 ng/cm^2 ($1.25 \times 10^{-9} \text{ mol/cm}^2$). Both mass changes are consistent with approximately single monolayers and a 1:1 reaction stoichiometry. The reaction product is the hydrochloride salt as shown in Scheme I.

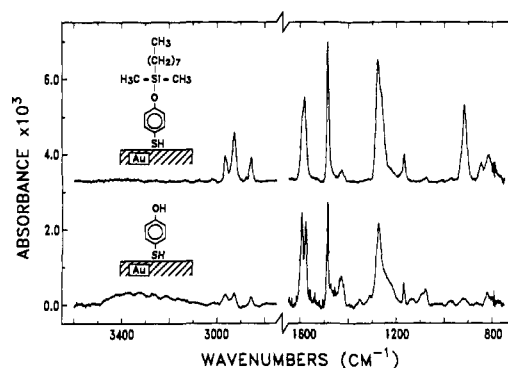


Figure 2. FTIR-ERS spectra of (bottom) a monolayer of 4-HTP confined to a Au substrate and (top) the product of the vapor-phase reaction between 4-HTP and $[\text{CH}_3(\text{CH}_2)_7](\text{CH}_3)_2\text{SiCl}$. After reaction, absorptions in the methyl and methylene stretching region ($2975\text{--}2850 \text{ cm}^{-1}$) are enhanced, and a new absorption arising from the symmetric Si-phenoxy stretch is present at 918 cm^{-1} . The two overlapping bands at 1277 and 1260 cm^{-1} result from the asymmetric Si-phenoxy stretch and the symmetric $\text{H}_3\text{C-Si-CH}_3$ deformation, respectively. Also, notice that the phenolic O-H stretch originally present at 3342 cm^{-1} has disappeared. The top spectrum is vertically offset for clarity. All spectra were obtained with p-polarized light incident on the substrate at 85° off the surface normal. Each spectrum is the sum of 256 individual spectra.

Between 410 and 530 min, the SAW device is exposed to a mixed $[\text{CH}_3(\text{CH}_2)_7](\text{CH}_3)_2\text{SiCl}/\text{N}_2$ vapor, and the observed frequency shift again indicates multilayer condensation. A pure N_2 purge beginning at 530 min removes most of the condensed silane, leaving behind an additional mass of 229 ng/cm^2 ($1.25 \times 10^{-9} \text{ mol/cm}^2$, assuming formation of the hydrochloride salt of the product). These data clearly show that the coupling reaction between surface-confined 4-ATP and vapor phase $[\text{CH}_3(\text{CH}_2)_7](\text{CH}_3)_2\text{SiCl}$ is stoichiometric and confirm that a chemical reaction has occurred.⁷

Figure 2 shows the FTIR-ERS spectrum of a surface-confined monolayer of 4-HTP before and after exposure to $[\text{CH}_3(\text{C}-\text{H}_2)_7](\text{CH}_3)_2\text{SiCl}$. The bottom spectrum shows the characteristic absorptions for 4-HTP: the aromatic ring vibrations at 1596 , 1579 ,

(2) Nuzzo, R. G.; Allara, D. L. *J. Am. Chem. Soc.* **1983**, *105*, 4481.

(3) Bain, C. D.; Troughton, E. B.; Tao, Y.-T.; Evall, J.; Whitesides, G. M.; Nuzzo, R. G. *J. Am. Chem. Soc.* **1989**, *111*, 321 and references therein.

(4) Thomas, R. C.; Sun, L.; Crooks, R. M.; Ricco, A. J. *Langmuir* **1991**, *7*, 620.

(5) Rubinstein, I.; Rishpon, J.; Sabatani, E.; Redondo, A.; Gottesfeld, S. *J. Am. Chem. Soc.* **1990**, *112*, 6135.

(6) The theoretical monolayer coverage of 4-ATP can be estimated at $1.4 \times 10^{-9} \text{ mol/cm}^2$ by assuming an ideal Au(111) surface, adsorption at 3-fold hollow sites (Bard, A. J., The University of Texas, Austin, personal communication), and an appropriate surface roughness factor. For the substrates used here the measured surface roughness factor is 1.8 ± 0.3 , in agreement with independently prepared Au/Ti/Si substrates (Rubinstein, I., The Weizman Institute of Science, private communication).

(7) When the silane coupling agent is allowed to contact a naked Au surface, no significant adsorption occurs.

1489, and 1431 cm^{-1} , the broad C–O stretching peak at 1278 cm^{-1} , and the broad phenolic O–H stretching peak centered at 3342 cm^{-1} . The small peaks between 2975 and 2850 cm^{-1} are due to a small amount of hydrocarbon contamination. The top part of Figure 2 shows the spectrum for the 4-HTP surface after exposure to the silane. In the high-frequency region, the phenolic O–H band originally present at 3342 cm^{-1} has disappeared, and stronger absorptions between 2975 and 2850 cm^{-1} indicate the presence of the hydrocarbon portion of the silane coupling agent. In the low-frequency region, the somewhat enhanced aromatic ring stretches are still present at 1585 and 1486 cm^{-1} ,⁸ but there is a new absorption at 918 cm^{-1} arising from the symmetric Si–phenoxy stretching mode of the reaction product, Scheme 1.⁹ The two overlapping bands at 1277 and 1260 cm^{-1} result from the asymmetric Si–phenoxy stretch and the symmetric $\text{H}_3\text{C–Si–CH}_3$ deformation, respectively.⁹

Ellipsometric results⁴ are in accord with the SAW and FTIR-ERS experiments. The average measured thickness of three vapor-deposited 4-HTP layers is $5.8 \pm 0.8 \text{ \AA}$, which increases to $12.5 \pm 1.2 \text{ \AA}$ after reaction with $[\text{CH}_3(\text{CH}_2)_7](\text{CH}_3)_2\text{SiCl}$. Similar results are found for surface-confined 4-ATP before ($7.4 \pm 0.9 \text{ \AA}$) and after ($12.1 \pm 1.2 \text{ \AA}$) exposure to $[\text{CH}_3(\text{CH}_2)_7](\text{CH}_3)_2\text{SiCl}$. These data show that both reactants and products are present at approximately monolayer coverage. Since we do not know the orientation of the adsorbates, it is difficult to infer theoretical thicknesses for the organic monolayers, but the trend toward thicker layers is expected.

To summarize, we have demonstrated that well-characterized reactions occur between surface-confined monolayers and vapor-phase reactants at atmospheric pressure. These reaction conditions provide an important link between solution and ultra-high-vacuum studies. Real-time SAW experiments, FTIR-ERS, and ellipsometry demonstrate that the vapor-phase coupling reactions between surface-confined 4-HTP or 4-ATP and $[\text{CH}_3(\text{CH}_2)_7](\text{CH}_3)_2\text{SiCl}$ result in monolayer coverages of stoichiometric reaction products. Moreover, experiments with other coupling agents, $[\text{CH}_3(\text{CH}_2)_n](\text{CH}_3)_2\text{SiCl}$ ($n = 0, 2$), show appropriate attenuations in mass, methylene stretching absorption intensity, and thickness, further supporting our conclusions. At present, we have no evidence that either the reactants or products are highly organized, but experiments are in progress to extend this study to other vapor-phase coupling reactions that may lead to such structures.

Acknowledgment. The excellent technical assistance of Barbara L. Wampler is gratefully acknowledged. Experiments at the University of New Mexico are supported by the Sandia–University Research Program (DOE) and the National Science Foundation (CHE-90146566). R.M.C. gratefully acknowledges a Society of Analytical Chemists of Pittsburgh Starter Grant Award and an Office of Naval Research Young Investigator Award. Research at Sandia National Laboratories is supported by the U.S. DOE under Contract No. DE-AC04-76DP00789.

Registry No. Au, 7440-57-5; $[\text{CH}_3(\text{CH}_2)_7](\text{CH}_3)_2\text{SiCl}$, 18162-84-0; 4-HTP, 637-89-8; 4-ATP, 1193-02-8.

Supplementary Material Available: Details of the SAW, ellipsometry, and synthesis and spectral characterization of solution analogues of the surface-confined reactants and products (5 pages). Ordering information is given on any current masthead page.

(8) Enhancements in ring mode absorptions after reaction are most likely the result of orientational changes that are consistent with the surface selection rules for FTIR-ERS; see: (a) Greenler, R. G. *J. Chem. Phys.* **1966**, *44*, 310. (b) Greenler, R. G. *J. Chem. Phys.* **1969**, *50*, 1963. (c) Porter, M. D. *Anal. Chem.* **1988**, *60*, 1143A.

(9) The band assignments for surface-confined $\text{HS}(\text{C}_6\text{H}_4)\text{OSi}(\text{CH}_3)_2[(\text{C}_6\text{H}_2)_7\text{CH}_3]$ have been confirmed by comparison to an authentic sample of $(\text{C}_6\text{H}_5)\text{OSi}(\text{CH}_3)_2[(\text{CH}_2)_7\text{CH}_3]$. Details of the synthesis and the NMR and FTIR spectral analyses are given in the supplementary material. (a) Anderson, D. R. In *Analysis of Silicones*; Smith, A. L., Ed.; Wiley: New York, 1974; Chapter 10. (b) Bellamy, L. J. *The Infra-red Spectra of Complex Molecules*, 3rd ed.; Chapman and Hall: London, 1975; Chapter 20.

Molecular Orbital Theory Calculations of Aqueous Solvation Effects on Chemical Equilibria

Christopher J. Cramer*

U.S. Army Chemical Research Development and Engineering Center
Aberdeen Proving Ground, Maryland 21010-5423

Donald G. Truhlar*

Department of Chemistry, Supercomputer Institute, and Army High-Performance Computing Research Center
University of Minnesota
Minneapolis, Minnesota 55455-0431

Received July 16, 1991

Molecular modeling techniques¹ have advanced to the point where computational chemistry can predict the relative energies of many interesting structures, intermediates, and possible reaction products. Parametric models^{2–4} based on semiempirical molecular orbital theory are especially useful for treating substituent effects and evaluating competing structures; for reactions in aqueous solution, though, there is considerably uncertainty about the applicability of the calculated results since the computational models do not include the solvent. One way to improve on this situation is to combine these models with the local-field SCF approach.⁵ In this spirit, we have recently proposed and calibrated a new parameterized model,⁶ called AM1-SM1, in which an aqueous "solvation model" (SM1) is added to the Fock operator from neglect-of-diatom-differential-overlap⁷ semiempirical molecular orbital theory using the Austin model 1 (AM1)⁸ parameterization for the solute. SM1 treats the solvent as a bulk continuum with a generalized Born model^{8,9} with dielectric screening for the polarization energy (we use a model in which the solute cavity from which dielectric is excluded is composed of superimposed spheres^{9,10}) and with surface tension terms¹¹ (based on the solvent-accessible surface area¹²) for cavity and dispersion effects. Parameters are available⁶ for 298 K for solutes containing H, C, N, O, F, S, Cl, Br, and I. The theory is especially promising because it requires considerably less in the way of computational resources than simulations with explicit inclusion of a large number of water molecules,¹³ yet *at the same time* it allows for solvent-induced changes in the solute charge distribution.

Here we report the first tests of AM1-SM1 for the effect of solvation on reactive equilibria, in particular for acid–base proton transfer reactions, prototropic tautomerizations, and the rotameric isomerization of the peptide linkage. We define

$$\Delta\Delta G^\circ_{g\rightarrow aq} = \Delta G^\circ_{aq} - \Delta G^\circ_g \quad (1)$$

where ΔG° is the standard-state (1 M) free energy change for

(1) Naray-Szabo, G.; Surjan, P. R.; Angyan, J. G. *Applied Quantum Chemistry*; Reidel: Dordrecht, 1987.

(2) Dewar, M. J. S.; Thiel, W. *J. Am. Chem. Soc.* **1977**, *99*, 4899, 4907.

(3) (a) Dewar, M. J. S.; Zoebisch, E. G.; Healy, E. F.; Stewart, J. J. P. *J. Am. Chem. Soc.* **1985**, *107*, 3902. (b) Dewar, M. J. S.; Dieter, K. M. *J. Am. Chem. Soc.* **1986**, *108*, 8075.

(4) Stewart, J. J. P. *J. Comput. Chem.* **1989**, *10*, 209, 221.

(5) For reviews, see: (a) Tapia, O. In *Quantum Theory of Chemical Reactions*; Daudel, R., Pullman, A., Salem, L., Viellard, A., Eds.; Reidel: Dordrecht, 1980; Vol. 2, p 25. (b) Tomasi, J.; Alagona, G.; Bonaccorsi, R.; Ghio, C. In *Modelling of Structure and Properties of Molecules*; Maksić, Z. B., Ed.; Horwood: Chichester, 1987; p 330.

(6) Cramer, C. J.; Truhlar, D. G. *J. Am. Chem. Soc.*, in press.

(7) (a) Pople, J. A.; Santry, D. P.; Segal, G. A. *J. Chem. Phys.* **1965**, *43*, 5129. (b) Pople, J. A.; Beveridge, D. L. *Approximate Molecular Orbital Theory*; McGraw-Hill: New York, 1970.

(8) (a) Houtjink, G. J.; de Boer, E.; van der Meij, P. H.; Weijland, W. P. *Recl. Trav. Chim. Pays-Bas* **1956**, *75*, 487. (b) Peradejordi, *Cah. Phys.* **1963**, *17*, 393.

(9) Still, W. C.; Tempczak, A.; Hawley, R. C.; Hendrickson, T. *J. Am. Chem. Soc.* **1990**, *112*, 6127.

(10) (a) Miertus, S.; Scrocco, E.; Tomasi, J. *J. Chem. Phys.* **1981**, *55*, 117. (b) Bonaccorsi, R.; Cimraglia, R.; Tomasi, J. *J. Comput. Chem.* **1983**, *4*, 567.

(11) Hermann, R. B. *J. Phys. Chem.* **1972**, *76*, 2754.

(12) Lee, B.; Richards, F. M. *J. Mol. Biol.* **1971**, *55*, 379.

(13) (a) Watts, R. O.; Clementi, E.; Fromm, J. *J. Chem. Phys.* **1974**, *61*, 2550. (b) Beveridge, D. L.; DiCapua, F. M. *Annu. Rev. Biophys. Biophys. Chem.* **1989**, *18*, 431. (c) Jorgensen, W. L. *Chemtracts: Org. Chem.* **1991**, *4*, 91.